A simple approach for predicting soil water characteristic curve of clayey soils using pore size distribution data

Wei Yan[1,*], *Emanuel Birle*[1], and *Roberto Cudmani*[1]

[1]Technical University of Munich, Center for Geotechnics, Franz-Langinger-Str. 10, 81245 Munich, Germany

Abstract. The soil water characteristic curve (SWCC) of soils can be derived from the measured pore size distribution (PSD) data by applying capillary models. This method is limited for clayey soils due to the PSD changes during SWCC testing. In this study, a suction-dependent multimodal PSD model based on probability theory is developed and used to derive SWCC. The model is validated by simulating the drying branches of SWCCs of four compacted Lias Clay samples with different initial states. A good consistency between the measured and predicted SWCC is shown.

1 Introduction

Soil Water Characteristic Curve (SWCC) describes the relationship between matric suction and the degree of saturation of a soil, which plays a key role in unsaturated soil mechanics [1]. Important soil properties, for example, the unsaturated hydraulic conductivity, are highly related to SWCC. The SWCC of a soil is characterized by its pore size distribution (PSD), regarding the pore structure of the soil as a bundle of circular tubes. The PSD of a soil can be transformed to its SWCC based on the capillary law [2]. However, this simple method possibly oversimplifies the transformation of PSD to SWCC due to the heterogeneity of the soil structure, especially for clayey soils [3,4]. Therefore, the directly measured SWCC can be significantly different from the SWCC transformed from PSD, particularly in low suction range. The inaccurate prediction of SWCC based on the capillary law is mainly caused by ignoring the changes in pore structure during SWCC testing. The SWCC is measured at the entire suction range, whereas the PSD is usually determined by mercury intrusion porosimetry (MIP) at a specific state after the sample is prepared and freeze-dried. In other words, the pore size distribution of the soil is variable during SWCC testing and constant for MIP tests.

This study is aimed to develop a simple approach to accurately predict the SWCC of clayey soils using the PSD data. A suction-dependent multimodal probability model is developed to describe PSD changes during SWCC testing. Eventually, the model is validated by predicting the drying branches of SWCCs of four compacted Lias Clay samples with different initial states.

2 Theory

2.1 Direct transformation of PSD to SWCC

A mathematical definition for the pore radius r according to Scheidegger [5] is adopted in this study. The pore radius r denoted to a point inside the pore space is defined as the radius of the maximum sphere containing this point within the pore space (i.e., the sphere cannot touch the soil particle). It is not hard to find that the pore radius r is a non-negative random variable depending on the position of the point. According to probability theory, we have

$$\int_0^{+\infty} f(r)\,dr = 1. \tag{1}$$

Herein, $f(r)$ represents the pore size distribution of the soil, which is a continuous probability density function about the pore radius r. Considering that r is presented in the unit of Length L, the unit of $f(r)$ is L^{-1}. Following Juang & Holtz [6], the pore size density function can also be expressed in a dimensionless form as:

$$\int_0^{+\infty} \omega(r)\,\mathrm{dlog}\,r = 1, \tag{2}$$

where log r represents the base 10 logarithm of r. Comparing Eq. (1) and Eq. (2), we obtain a simple relationship between $f(r)$ and $\omega(r)$:

$$\omega(r) = (\ln 10) r f(r). \tag{3}$$

In this paper, $\omega(r)$ is used to represent PSD of soils for mathematical convenience.

Previous experimental evidences (e.g., [3,7-9]) have shown that the complicated pore structure of clayey soils can be bimodal and even multimodal. For instance, Romero et al. [3] observed two distinct sub porosities in the statically compacted Boom-Clay, i.e., the inter-

* Corresponding author: wei.yan@tum.de

aggregate and intra-aggregate porosities. More recently, Wang et al. [8] identified four pore families in bentonite MX80 during hydration. For a multimodal clayey soil, the whole pore structure can be regarded as a superposition of individual overlapping sub porosities [10], each of which is described by a sub pore size distribution function $\omega_i(r)$ and occupies a volumetric fraction R_i. That means,

$$\omega(r) = \sum_{i=1}^{N} R_i\, \omega_i(r), \tag{4}$$

where N is a positive integer representing the modality number. Substituting Eq. (4) to Eq. (2) gives

$$\int_0^{+\infty} \sum_{i=1}^{N} R_i\, \omega_i(r)\, \mathrm{dlog}\, r = 1. \tag{5}$$

For each sub porosity, we have

$$\int_0^{+\infty} \omega_i(r)\, \mathrm{dlog}\, r = 1. \tag{6}$$

The volumetric fraction R_i of each sub porosity fulfils the following condition:

$$\sum_{i=1}^{N} R_i = 1. \tag{7}$$

From Eqs. (6) and (7), it is not hard to find that the requirement expressed in Eq. (5) is fulfilled. A unimodal pore size density function $\omega_i(r)$, derived from van Genuchten model, is proposed as following:

$$\omega_i(r) = \frac{(\ln 10) m_i (\alpha_i C/r)^{\frac{1}{1-m_i}}}{(1-m_i)\left[1+(\alpha_i C/r)^{\frac{1}{1-m_i}}\right]^{m_i+1}}, \tag{8}$$

where m_i $(0 < m_i < 1)$ and α_i $(\alpha_i > 0)$ are parameters determined by pore size distribution of each sub porosity. The constant C is determined by the capillary law:

$$C = 2T\cos\varphi, \tag{9}$$

where T is surface tension of water of 0.072 N/m at 25 °C, and φ is contact angle between water and soil ($\varphi \approx 0$) [1,2]. According to the capillary law, the relationship between pore radius r and the suction s can be expressed as:

$$r = \frac{C}{s}. \tag{10}$$

Substituting Eq. (8) into Eq. (4), a general multimodal PSD model gives:

$$\omega(r) = \sum_{i=1}^{N} R_i \frac{(\ln 10) m_i (\alpha_i C/r)^{\frac{1}{1-m_i}}}{(1-m_i)\left[1+(\alpha_i C/r)^{\frac{1}{1-m_i}}\right]^{m_i+1}}. \tag{11}$$

Regarding the pore structure of a soil as a bundle of circular tubes, SWCC can be directly derived from the PSD function by applying the capillary law according to Fredlund & Xing [2]:

$$S_r = \int_s^{+\infty} \frac{1}{\ln 10}\, \omega\left(\frac{C}{s}\right)\frac{1}{s}\, ds. \tag{12}$$

Combining Eq. (11) and Eq. (12), the multimodal SWCC function directly transformed from the multimodal PSD function gives:

$$S_r = \sum_{i=1}^{N} R_i \left[1+(\alpha_i s)^{\frac{1}{1-m_i}}\right]^{-m_i}. \tag{13}$$

The desaturation of clayey soils consists of capillary and adsorptive processes [11]. At the high suction range, the SWCC is predominated by the relationship between adsorbed water and suction. Hence, the capillary law is not valid. In the proposed model [Eq. (13)], this mechanism is equivalently represented by a group of capillary tubes, which gives the same water content - suction relationship at the high suction range. That means, the whole pore structure of clayey soils (including the pore space occupied by adsorbed water) is regarded as an assemblage of capillary tubes, and its PSD is described by a general multimodal function in Eq. (4).

2.2 Transformation of PSD to SWCC considering the changes in PSD during SWCC testing

The direct transformation of PSD to SWCC requires a constant pore structure of the soil during the SWCC testing [12]. However, this assumption oversimplifies the mechanism in the soil fabric, especially for clayey soils. Simms & Yanful [12] measured the PSDs of several compacted clayey soils at different suction levels during SWCC testing and observed that the PSD of the clayey soils altered significantly with suction. More recently, Monroy et al. [13] detected the PSDs of compacted London clay at different suction levels during free-swelling testing. The results are shown in Fig. 1. The pore structure consists of a macro ($r \geq 20\ \mu m$) and a micro ($r \leq 20\ \mu m$) porosity. The PSD shows pronounced bimodal characterisation at the highest suction level of s = 996 kPa, while that at the saturation state of s = 0 kPa is almost unimodal. As suction decreases during hydration, the volumetric fraction of macro porosity decreases and the micro porosity increases. In addition, the predominate mean radius (pore radius at the peak) of macro porosity is almost constant, whereas that of the micro porosity gradually increases due to the swelling of aggregates. Consequently, the PSD variation during SWCC testing must be taken into account when transforming PSD to SWCC.

In order to derive an accurate SWCC from PSD data, all the parameters of the multimodal PSD model [Eq. (11)] are assumed to be suction-dependent:

$$\begin{cases} R_i = R_i(s) \\ \alpha_i = \alpha_i(s) \\ m_i = m_i(s) \end{cases} . \quad (14)$$

That means, each parameter (R_i, α_i and m_i) in the multimodal PSD model is a function of suction. Thus, considering the condition of Eq. (7), Eq. (14) includes 3N - 1 independent functions. From Eqs. (11) and (14), a suction-dependent multimodal PSD function during SWCC testing gives:

$$\begin{cases} \omega(r) = \sum_{i=1}^{N} R_i \dfrac{(\ln 10) m_i (\alpha_i C/r)^{\frac{1}{1-m_i}}}{(1-m_i)\left[1+(\alpha_i C/r)^{\frac{1}{1-m_i}}\right]^{m_i+1}} \\ R_i = R_i(s) \\ \alpha_i = \alpha_i(s) \\ m_i = m_i(s) \end{cases} . \quad (15)$$

It is worth to point out that Eq. (15) fulfils the requirement of Eq. (2) at any suction level. The PSD detected by MIP can be expressed as:

$$\begin{cases} \omega(r) = \sum_{i=1}^{N} R_i \dfrac{(\ln 10) m_i (\alpha_i C/r)^{\frac{1}{1-m_i}}}{(1-m_i)\left[1+(\alpha_i C/r)^{\frac{1}{1-m_i}}\right]^{m_i+1}} \\ R_i = R_i(s_0) \\ \alpha_i = \alpha_i(s_0) \\ m_i = m_i(s_0) \end{cases} . \quad (16)$$

where s_0 represents the suction in the soil before freeze-drying. Applying the capillary law in Eq. (10) to Eq. (15), the multimodal SWCC derived from the suction-dependent PSD model gives:

$$\begin{cases} S_r = \sum_{i=1}^{N} R_i \left[1+(\alpha_i s)^{\frac{1}{1-m_i}}\right]^{-m_i} \\ R_i = R_i(s) \\ \alpha_i = \alpha_i(s) \\ m_i = m_i(s) \end{cases} . \quad (17)$$

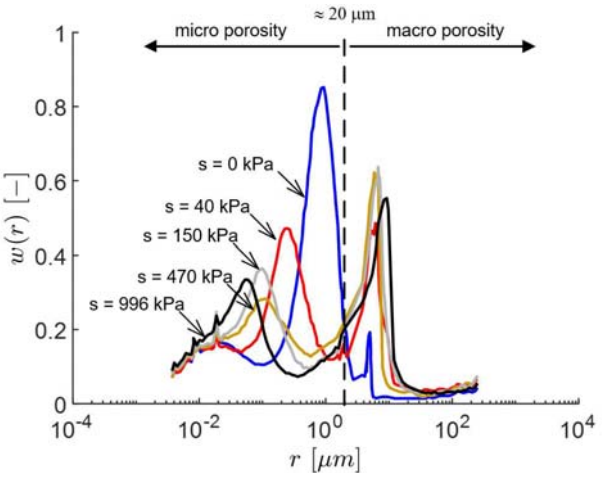

Fig. 1. Changes in the PSD of statically compacted London Clay along a free-swelling path (data adapted from [13])

3 Validation and discussion of the proposed model

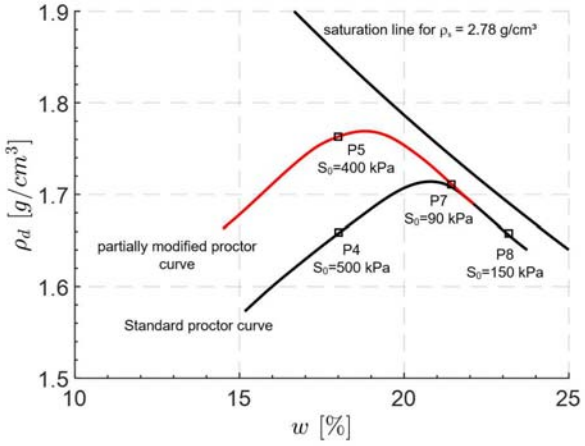

Fig. 2. Initial states of dynamically compacted Lias Clay samples (data adapted from [4])

Table 1. Mineralogical composition of Lias Clay (data adapted from [4])

Clay Mineral	percentage
smectite	1
Muscovite / illite	62
Kaolinite	23
Vermiculite	0
chlorite	14

Birle [4] prepared a set of samples of Lias clay, which were dynamically compacted to different initial densities at different water contents by using standard and modified (with relative higher compaction energy) proctor tests. The mineralogical composition of the soil is shown in Tab. 1. The soil is a medium plastic clay with a plastic limit w_p of 19.5% and a liquid limit w_L of 46.5%. The particle density of the soil is 2.78 g/cm³. Four initial states (P4, P5, P7 and P8) are shown in Figure 2, and two samples were prepared for each initial state. One of the two samples was used for MIP test, and the other for SWCC measurement.

For PSD measurements, the samples were freeze-dried at the initial state and thereafter set into mercury intrusion porosimetry. Thus, the measured PSD describes the pore structure of the sample at the initial suction level s_0. The detected mercury intrusion curves and the PSD curves are shown in Figure 3a and 3b, respectively. For the sample P4 with the highest initial suction s_0 = 500 kPa, the PSD curve shows a significant bimodal characterization, while other PSDs are almost unimodal. Therefore, a bimodal model (N = 2) is sufficient to describe the PSD:

$$\omega(r) = \sum_{i=1}^{2} R_i \frac{(\ln 10) m_i (\alpha_i C/r)^{\frac{1}{1-m_i}}}{(1-m_i)\left[1+(\alpha_i C/r)^{\frac{1}{1-m_i}}\right]^{m_i+1}}. \quad (18)$$

The parameters of the bimodal PSD model for each sample are individually determined by using the measured PSD data, which are shown in Tab. 2. Details of the parameter determination method is described by Yan et al. [14]. Figures 4a and 4b show the predicted mercury intrusion curves and the PSD curves, respectively. A good agreement between the measurements and the predictions is observed.

Table 2. parameters for the bimodal PSD model

	P4	P5	P7	P8
R_1 [-]	0.22	0.08	0.05	0.01
m_1 [-]	0.47	0.44	0.46	0.47
m_2 [-]	0.41	0.33	0.33	0.29
α_1 [kPa^{-1}]	1/5.5	1/200	1/63	1/25
α_2 [kPa^{-1}]	1/3.5e3	1/5e3	1/2.4e3	1/1.3e3

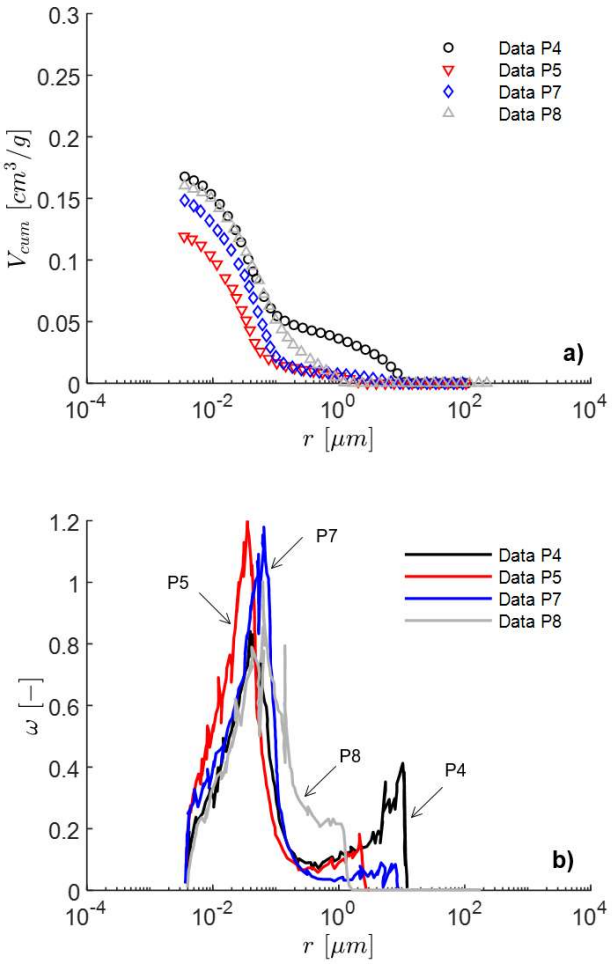

Fig. 3. a) measured mercury intrusion curves by MIP tests b) measured PSD curves (data adapted from [4])

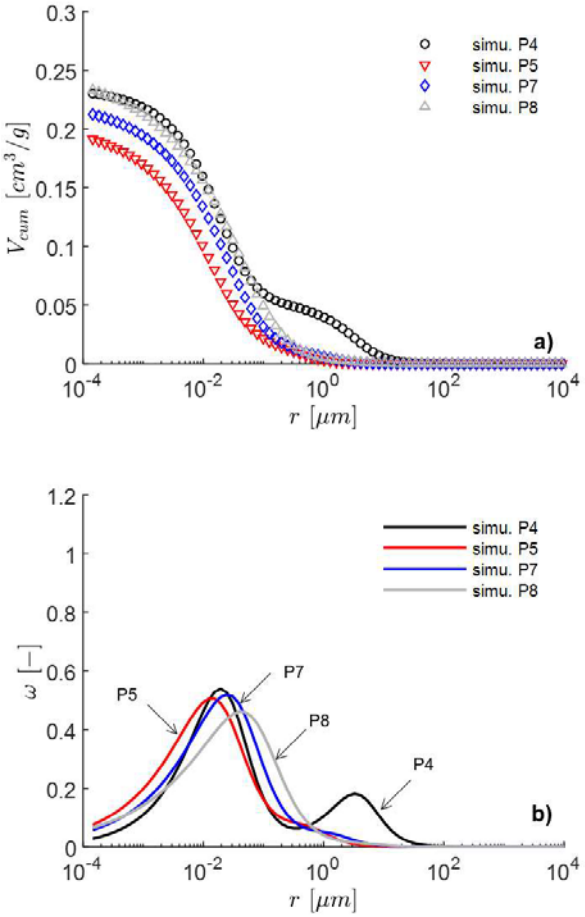

Fig. 4. a) predicted mercury intrusion curves for the MIP tests b) predicted PSD curves

The SWCC of the compacted Lias clay samples was measured by axis translation technique. Details of the sample preparation and testing procedure are described by Birle [4]. Starting from the initial states after compaction the samples were first wetted and then dried for the determination of the drying branch of water retention curve, which are shown in Fig. 5 (for P4 and P5) and Fig. 6 (for P7 and P8). For the different initial states, the measured SWCCs of the samples are similar and demonstrate unimodal characterization.

Based on Eq. (13) and the parameters in Tab. 2, SWCCs of the samples can be directly derived from their PSD (see Figs. 5 and 6). It shall be noted that the part of PSD curve at the very small radius range is obtained by extrapolation of the measured PSD data based on the proposed probability density function for the micro sub porosity [Eq. (8)]. This part of PSD curve corresponds to the directly derived SWCC at the high suction range, representing the adsorbed water. As shown in Figs. 5 and 6, the directly derived SWCCs at the high suction range are close to the measurements. A similar result can also be found in Romero et al. [3]. However, Figures 5 and 6 show the pronounced discrepancies between the measured SWCCs and the SWCCs directly derived from PSD at the low suction range. Especially, for the sample P4, the SWCC derived from PSD exhibits a distinct bimodal characterisation, while the measured SWCC is unimodal.

For the samples compacted at the dry side with high suction level (e.g., P4 and P5), the aggregates and macro pores in the soil are well developed before freeze-drying. Therefore, for the SWCC directly derived from PSD, the desaturation rate is high in the low suction range due to the macro pores in the pore structure. However, during SWCC testing, the sample is saturated at low suction level, leading to swelling of the aggregates and a significant reduction of macro pores. Thus, the desaturation rate at low suction range is smaller and the air entry value is greater than that of the SWCC directly derived from PSD curve.

For the samples compacted at the wet side with relative low suction level and high degree of saturation (e.g., P7 and P8), the PSD before freeze-drying is almost unimodal. However, since PSD changes during SWCC testing (suction increases during the drying branch of the SWCC), a gap between the measured SWCC and SWCC directly derived from PSD is observed, but less pronounced in comparison with the samples compacted at the dry side.

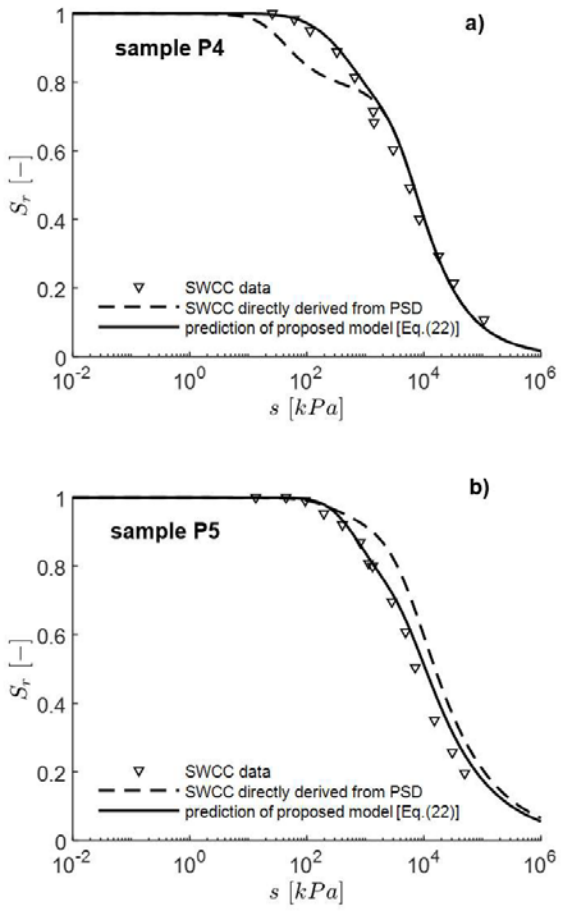

Fig. 5. comparison of the SWCC directly derived from PSD and the predicted SWCC by the proposed model a) sample P4, s_0=500 kPa. b) sample P5, s_0=400 kPa (data adapted from [4])

Consequently, the SWCC of the clayey soil cannot be accurately predicted by directly transforming the measured PSD. Because the pore structure changes with suction during the SWCC testing, while the PSD determined by MIP tests only describes the pore structure of the soil at the suction level before freeze-drying. Thus, the improved model in Eqs. (15) and (17) is adopted to predict the SWCCs by using PSD data.

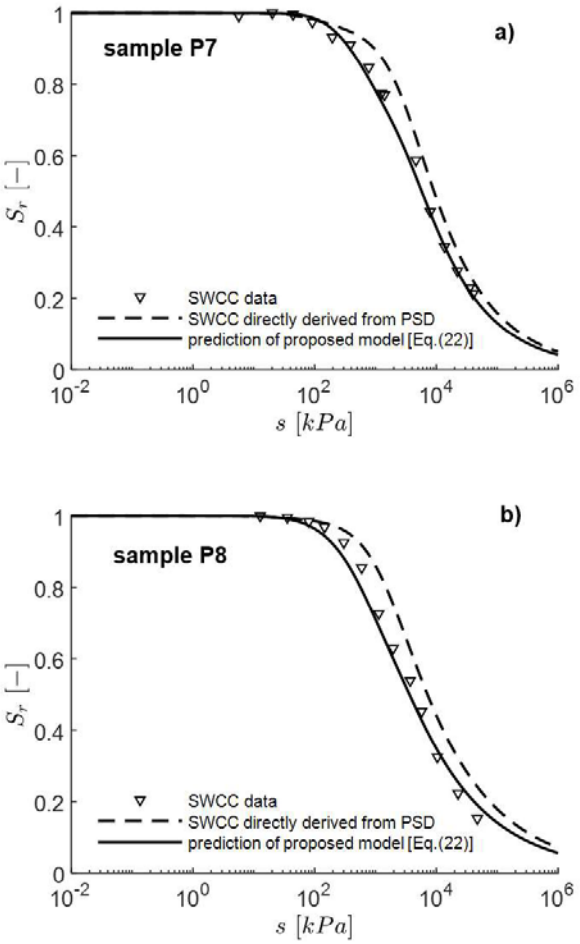

Fig. 6. comparison of the SWCC directly derived from PSD and the predicted SWCC by the proposed model a) sample P7, s_0=90 kPa. b) sample P8, s_0=150 kPa (data adapted from [4])

It must be emphasized that the condition expressed in Eq. (14) differs for each sample, since the samples were compacted at different initial states. For the aim of simplicity, we may assume that only the parameters R_i vary during SWCC testing, and the evolution with suction is identical for all the samples. That means, the macro volumetric fraction R_1 can be related to initial suctions of the samples (see Fig. 7). Due to the lack of data in the suction range greater than 500 kPa, the R_1 of the sample P4 (s_0 = 500 kPa) is regarded as the maximum macro volumetric fraction. Therefore, the evolution of R_1 is modelled with the following exponential equation:

$$R_1 = 0.22[1 - \exp(-0.002s)]. \quad (19)$$

According to Eq. (7), the micro volumetric fraction R_2 gives:

$$R_2 = 1 - 0.22[1 - \exp(-0.002s)]. \quad (20)$$

Thus, the suction-dependent PSD during SWCC testing for the samples can be expressed as:

$$\begin{cases} \omega(r) = \sum_{i=1}^{2} R_i \dfrac{(\ln 10) m_i (\alpha_i C/r)^{\frac{1}{1-m_i}}}{(1-m_i)\left[1+(\alpha_i C/r)^{\frac{1}{1-m_i}}\right]^{m_i+1}} \\ R_1 = 0.22[1-\exp(-0.002s)] \\ R_2 = 1-0.22[1-\exp(-0.002s)] \end{cases}, \quad (21)$$

Applying the capillary law to Eq. (21), the SWCC model for the samples gives:

$$\begin{cases} S_r = \sum_{i=1}^{2} R_i \left[1+(\alpha_i s)^{\frac{1}{1-m_i}}\right]^{-m_i} \\ R_1 = 0.22[1-\exp(-0.002s)] \\ R_2 = 1-0.22[1-\exp(-0.002s)] \end{cases}. \quad (22)$$

The parameters m_i and α_i for each sample, which are assumed to be constant during SWCC testing, are again adopted from Tab. 2. Figure 5 and 6 show a good consistency between the measured and predicted SWCC. For the sample compacted at the dry side with relative high suction (P4 and P5), the predicted SWCCs also demonstrate a unimodal characterization. For the samples compacted at the wet side with relative low suction (P7 and P8), the air entry value predicted by the proposed improved model is more accurate than the direct transformation.

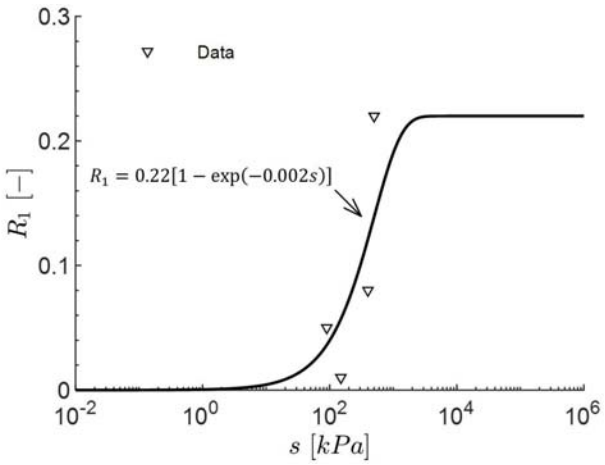

Fig. 7. evolution of the volumetric fraction of macro porosity R_1 with suction for compacted Lias Clay

4 Conclusion

For clayey soils, the SWCC directly derived from the PSD are usually different from the measured SWCC data. The PSD detected by MIP tests describes the pore structure at the suction level before freeze-drying, while the PSD of clayey soils changes with suction during SWCC testing, which is an important aspect when transforming PSD to SWCC. In this study, a suction-dependent multimodal PSD model for clayey soils is developed and used to predict SWCC. The model is validated by reproducing the SWCCs of compacted Lias – clay samples by using the bimodal PSD data. A good agreement between the predicted and measured SWCC is observed.

Acknowledgements

The financial support of the China Scholarship Council with grant number 201608080128 is greatly acknowledged by the first Author.

References

1. D. G. Fredlund & H. Rahardjo (1993). *Soil mechanics for unsaturated soils*. John Wiley & Sons.
2. D. G. Fredlund & A. Xing (1994). Equations for the soil-water characteristic curve. CAN GEOTECH J **31** (4):521-532
3. E. Romero, A. Gens, A. Lloret (1999). Water permeability, water retention and microstructure of unsaturated compacted Boom clay. ENG GEOL **54** (1-2):117-127
4. E. Birle (2011). Geohydraulische Eigenschaften verdichteter Tone unter besonderer Berücksichtigung des ungesättigten Zustandes. Technische Universität München.
5. A. E. Scheidegger (1958). The physics of flow through porous media. SOIL SCI **86** (6):355
6. C. Juang & R. Holtz (1986). A probabilistic permeability model and the pore size density function. INT J NUMER ANAL MET **10** (5):543-553
7. E. E. Alonso, N. M. Pinyol, A. Gens (2013). Compacted soil behaviour: initial state, structure and constitutive modelling. GEOTECHNIQUE **63** (6):463-478. doi:*10.1680/geot.11.P.134*
8. Q. Wang, Y.-J. Cui, A. Minh Tang, L. Xiang-Ling, Y. Wei-Min (2014). Time- and density-dependent microstructure features of compacted bentonite. SOILS FOUND **54** (4):657-666. doi:*10.1016/j.sandf.2014.06.021*
9. Y. Gao, D. a. Sun, Z. Zhu, Y. Xu (2019). Hydromechanical behavior of unsaturated soil with different initial densities over a wide suction range. ACTA GEOTECH **14** (2):417-428
10. P. J. Ross & K. R. Smettem (1993). Describing soil hydraulic properties with sums of simple functions. SOIL SCI SOC AM J **57** (1):26-29
11. N. Lu (2016). Generalized soil water retention equation for adsorption and capillarity. J GEOTECH GEOENVIRON **142** (10):04016051
12. P. Simms & E. Yanful (2002). Predicting soil—Water characteristic curves of compacted plastic soils from measured pore-size distributions. GEOTECHNIQUE **52** (4):269-278
13. R. Monroy, L. Zdravkovic, A. Ridley (2010). Evolution of microstructure in compacted London Clay during wetting and loading. GEOTECHNIQUE **60** (2):105-119. doi:*10.1680/geot.8.P.125*
14. W. Yan, E. Birle, R. Cudmani (2021). A new framework to determine general multimodal soil water characteristic curves. submitted to Acta geotechnica